The material presented below is intended as a review only. A full length paper has been submitted for publication in IEEE/MTT (May 1992).

DOUBLE-SLOT ANTENNAS ON EXTENDED HEMISPHERICAL DIELECTRIC LENSES

Daniel F. Filipovic, Steve J. Gearhart, Brian K. Kormanyos and Gabriel M. Rebeiz

NASA/Center for Space Terahertz Technology
Electrical Engineering and Computer Science Department
University of Michigan
Ann Arbor, MI 48109-2122

ABSTRACT

An investigation of the coupling efficiencies to a gaussian-beam of a double-slot antenna on a hyperhemispherical lens is presented. It is shown that both lenses couple equally well to an appropriate gaussian beam (about 80%). The radiation patterns of both lenses with a double-slot antenna are computed using the ray-tracing method. The experimental radiation patterns are presented and show close agreement to the theoretically computed patterns.

I. INTRODUCTION

The use of a hemispherical lens with an attached extension length can greatly improve coupling to a gaussian-beam system. In optical theory, an extension length of r/n is used, and this extended lens is termed a hyperhemispherical lens. This extension length was chosen since it satisfies the sine condition, which is where first-order aberrations are removed [1]. The hyperhemispherical lens was borrowed into the millimeter-wave field [2,3,4], but it was found that radiation patterns from these lenses were very broad and even multi-lobed in some cases. The hyperhemispherical lens is capable of coupling well to a gaussian-beam system. However, it couples most efficiently to a converging beam and not to a plane wave. Recently, several researchers showed that a narrow, diffraction-limited beam could be achieved by putting the antennas on an elliptical lens [5,6]. The same effect was also found by taking a hyperhemispherical lens and adding a planar extension to it [7]. Figure 1 shows that the focus of this longer extension length lens superimposes exactly on the second focus of an elliptical lens. It is known from optical theory that a plane wave converges to the second focus of an ellipse, and therefore a lens with this extension length is simply a close geometrical approximation to an elliptical lens. The validity of this approximation depends on the maximum allowed phase tolerance. For high dielectric constants (see Fig. 1) and relatively low frequencies, the phase difference becomes small and the approximation is valid. Generally, for lens diameter of 12.5mm, ϵ larger than 4, and frequencies less than 300GHz, the approximation is very good.

II. THEORETICAL AND EXPERIMENTAL PATTERNS

The theoretical radiation patterns are computed using a ray-tracing technique [9]. First, the feed antenna pattern into the dielectric is calculated using standard far-field methods. Figure 2 shows the calculated radiation patterns for a double-slot antenna with $L = 0.28\lambda_{air}$ and $d = 0.16\lambda_{air}$. These parameters were chosen to result in a symmetric pattern inside the dielectric and a low cross-polarization in the 45°-plane. Ray-tracing is then used to calculate the electric field distribution across the aperture plane (Fig. 3). In this method, the fields are decomposed into TE/TM components at the lens/air interface, and the appropriate transmission formulas are used for each mode. The power reflected into the substrate is neglected in this analysis. A diffraction integral over the aperture then yields the far-field pattern from the lens. Experimental measurements were performed at 246GHz on a 13.7 mm diameter silicon lens (ϵ=11.7) with the double-slot antenna as a feed. Different values of extension length were achieved by adding high-resistivity silicon wafers, resulting in 3 extension lengths: hyperhemispherical, intermediate, and elliptical (Fig. 3). Measured patterns at the elliptical focus (Fig. 4) demonstrate a gain of 28.6dB$\pm$0.3dB with relatively low sidelobes (-16dB). From the measured patterns, the resulting aperture efficiency (coupling to a plane wave) is 73%. The theoretical patterns calculated for this position are a bit wider than the measured patterns (Fig. 5). This discrepancy arises from the fact that rays at a certain angle end up hitting the critical angle at the lens/air interface, resulting in no transmission of rays after this point. This limits the aperture size and results in a wider theoretical pattern. Note that this discrepancy is only significant at the elliptical focus for lenses with high dielectric constants. Measured patterns at the elliptical focus for $\pm$10% of the

246GHz design frequency (Fig. 6) result in nearly the same gain, and therefore the double-slot antenna has good pattern bandwidth. The measured power at broadside is nearly the same from 222GHz-270GHz, also indicating good impedance bandwidth for the double-slot design. The measured patterns at the intermediate focus (Fig. 7) are similar to the elliptical focus, but with a gain of 24dB±0.3dB. In this case, the critical angle is not a problem, and there is close agreement between theory and experiment (Fig. 8). At the hyperhemispherical focus (Fig. 9), the pattern becomes very wide with a gain of 18.1dB±0.3dB and shows a multi-peak behaviour, as indicated by theory (Fig. 10). As will be seen later, this has no detrimental effect on the coupling efficiency to a converging beam. The ratio of the 246GHz measured received power at broadside for an elliptical lens and a hyperhemispherical lens was 10dB which is the same as the difference in the measured directivities. This indicates that no power is coupled to substrate modes that may arise in the flat wafers.

III. GAUSSIAN-BEAM COUPLING

In order to match the double-slot/extended hemisphere system to a gaussian beam, one could compute the electric field across the aperture and match this to a gaussian beam. Since we had already predicted the far-field amplitude and phase distributions, we chose to compute the coupling efficiency to a gaussian beam in the far-field (see Appendix). In this calculation, the power radiated by the slot antennas to the air-side (which is 11.5% of the total power) is taken into account, and no lens-air interface loss is considered. The power loss radiated to the air side could be reflected using an appropriately designed cavity at the expense of impedance bandwidth. Figure 11 gives the gaussian-beam parameters which

yield the highest coupling efficiency, and shows that all three focus positions are capable of coupling equally well to a gaussian beam. However, the non-elliptical foci require a converging wavefront, whereas the elliptical focus couples directly to a Gaussian beam with an equal phase wavefront. Note that equivalent gaussian-beam parameters in the near field may be found through a simple inverse Fourier transform. A gaussian beam experiment was performed at 246GHz, in which it was attempted to couple all the power coming out of a lens into the double-slot antenna. For the elliptical focus, the lens was placed at the minimum waist position, where the radius of curvature is infinite, indicating an equal phase wavefront. For the hyperhemispherical position, the lens was placed closer to the lens, at a position where there is a negative radius of curvature. The proper negative radius of curvature and position were computed knowing the gaussian-beam parameters from Figure 11. It was found that the ratio of powers with either focus is the same within experimental error ($\pm 4\%$), indicating that both the hyperhemispherical focus and the elliptical focus will match equally well to an appropriately designed gaussian-beam system. Similar measurements were done on a log-periodic antenna from 90-250GHz. The results are similar to those presented in this paper and have been submitted for publication in IRMMW (May 92).

IV. ACKNOWLEDGEMENTS

This work was supported by the NASA/Center for Space Terahertz Technology at the University of Michigan.

APPENDIX

The field representation of a Gaussian beam is of the form: $\mathbf{E}_{\mathrm{Gauss}}(\theta) = \hat{\epsilon}\ \exp^{-[\theta/\theta_0]^2}\ \exp^{j\pi[\theta/\theta_1]^2}$ The coupling efficiency between an antenna pattern and a gaussian beam is calculated using the formula [12,13]:

$$\eta_{Gauss} = \frac{|\iint[\hat{\epsilon}_{\mathrm{co}} \cdot \mathbf{F}(\theta,\phi)^2]\ \exp^{-(\theta/\theta_0)^2}\ \exp^{j\pi(\theta/\theta_1)^2}\ \sin\theta \mathrm{d}\theta\mathrm{d}\phi|^2}{\iint |\mathbf{F}(\theta,\phi)|^2 \sin\theta \mathrm{d}\theta\mathrm{d}\phi \iint \exp^{-2(\theta/\theta_0)^2} \sin\theta \mathrm{d}\theta\mathrm{d}\phi}$$

where $\mathbf{F}(\theta,\phi)$ is the far-field pattern of the antenna, and $\hat{\epsilon}_{co}$ is the co-pol unit vector. The value Θ_0 controls the amplitude term and Θ_1 controls the phasing term. These values are varied to optimize the coupling efficiency.

REFERENCES

[1] Born and Wolf, *Principles of Optics* , Permagon Press, New York, 1959, pp. 252-252.

[2] D.B. Rutledge, D.P. Neikirk and D.P. Kasilingam, "Integrated Circuit Antennas," *Infrared and Millimeter-Waves*, Vol. 10, K.J. Button, Ed., Academic Press, New York, 1983, pp. 1-90.

[3] D.B. Rutledge and M. Muha, "Imaging antenna arrays," *IEEE Trans. Antennas Propagat.*, Vol. AP-30, 1982, pp.535-540.

[4] J. Zmuidzinas, "Quasi-optical slot antenna SIS mixers," *IEEE Trans. on Microwave Theory Tech.*, accepted for publication Jan. 1992. Also presented at the *2nd Int. Symp. on Space Terahertz Technology*, CA, March 1991.

[5] A. Skalare, Th. de Graauw, and H. van de Stadt,"A Planar Dipole Array Antenna with an Elliptical Lens," *Microwave and Optical Tech. Lett.*, Vol. 4, No. 1, 1991, pp. 9-12. Also, "Millimeter and Submillimeter Studies of Planar Antennas," *First Int. Symp. on Space Terahertz Technology*, Ann Arbor, MI, March 1990, pp. 235-255.

[6] C.J. Adler, C.R. Brewitt-Taylor, R.J. Davis, M. Dixon, R.D. Hodges, L.D. Irving, H.D. Rees, J. Warner, and A.R. Webb, "Microwave and Millimeter-Wave Staring Array Technology," *IEEE MTT-S Int. Microw. Symp. Digest*, June 1991, pp. 1249-1252.

[7] T.H. Büttgenbach, "A Fixed Tuned Broadband Matching Structure for Submillimeter SIS Receivers," presented at the *Third Int. Symp. on Space Terahertz Technology*, Ann Arbor, MI, March 1992.

[8] A.E. Siegman, *Lasers*, University Science Books, New York, 1986.

[9] R.E. Collin, *Antennas and Radiowave Propagation*, McGraw-Hill, New York, 1985, pp. 190-199.

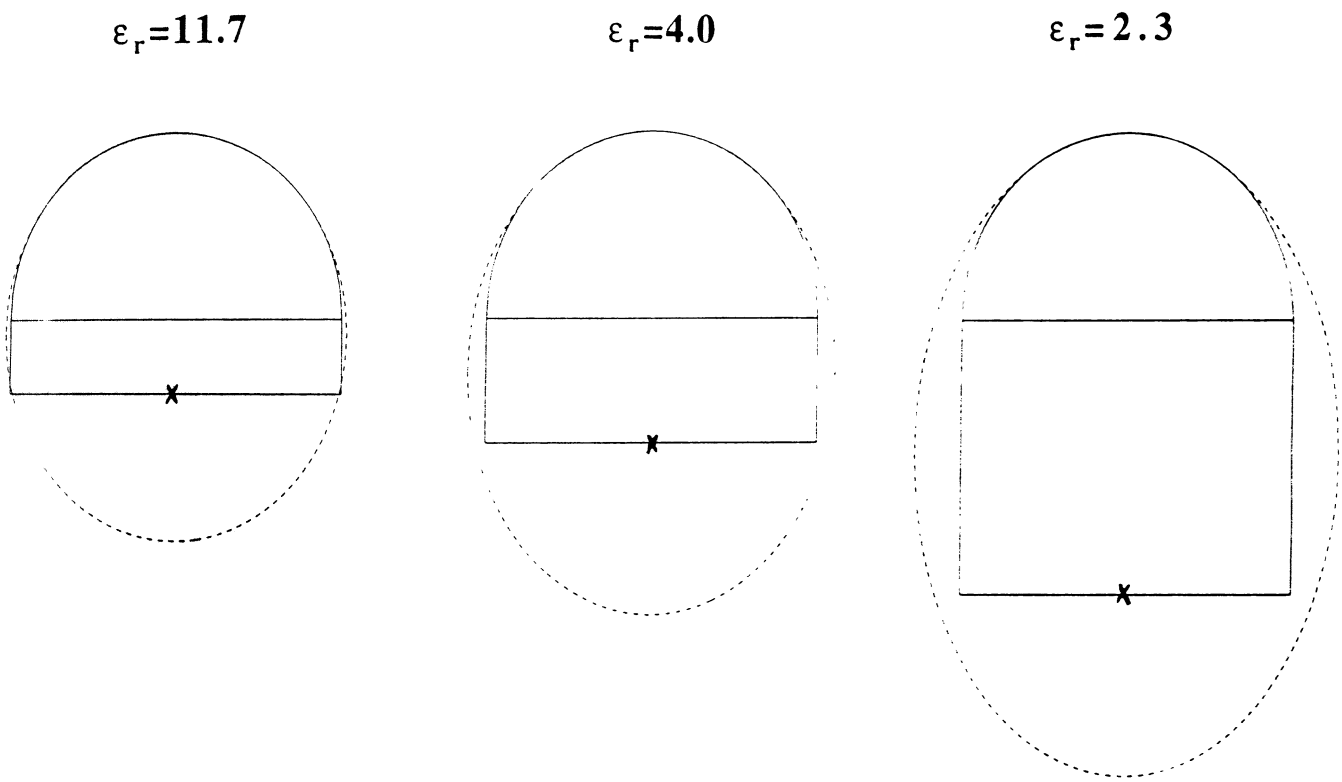

Figure 1: The synthesis of an elliptical lens from a hyperhemispherical lens and planar wafers. The extended hemisphere is a very good approximation to an elliptical lens at high dielectric constants.

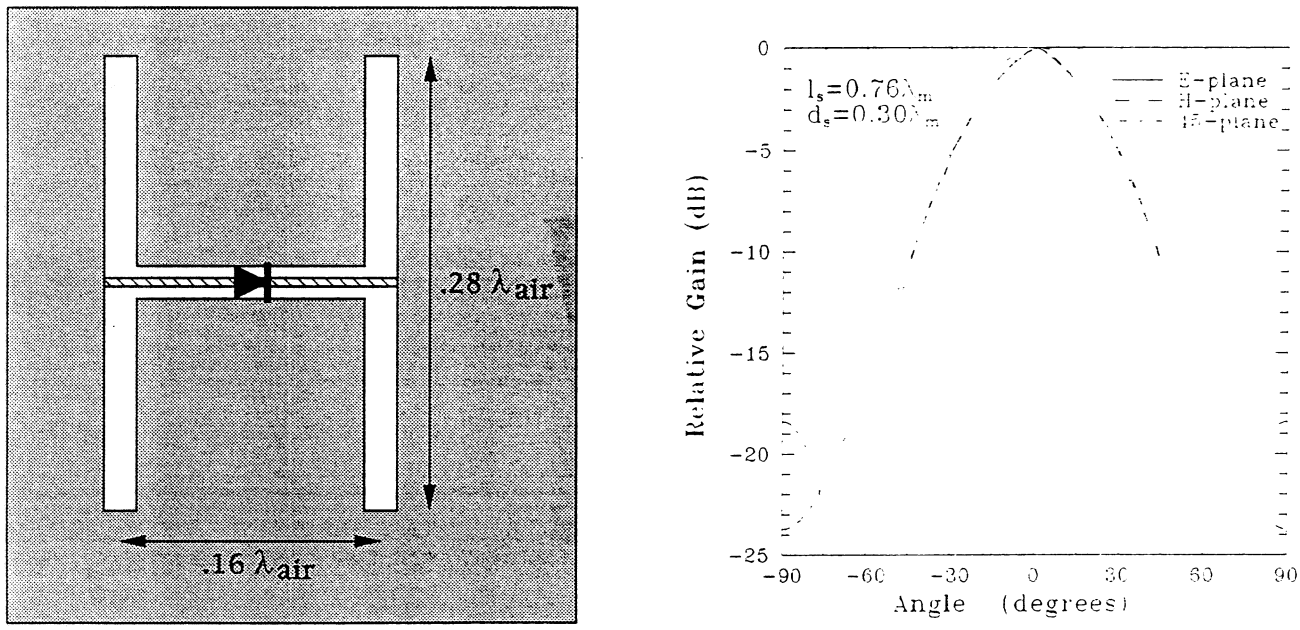

Figure 2: The double-slot antenna (left) and its radiation patterns into a silicon (ϵ=11.7) dielectric (right).

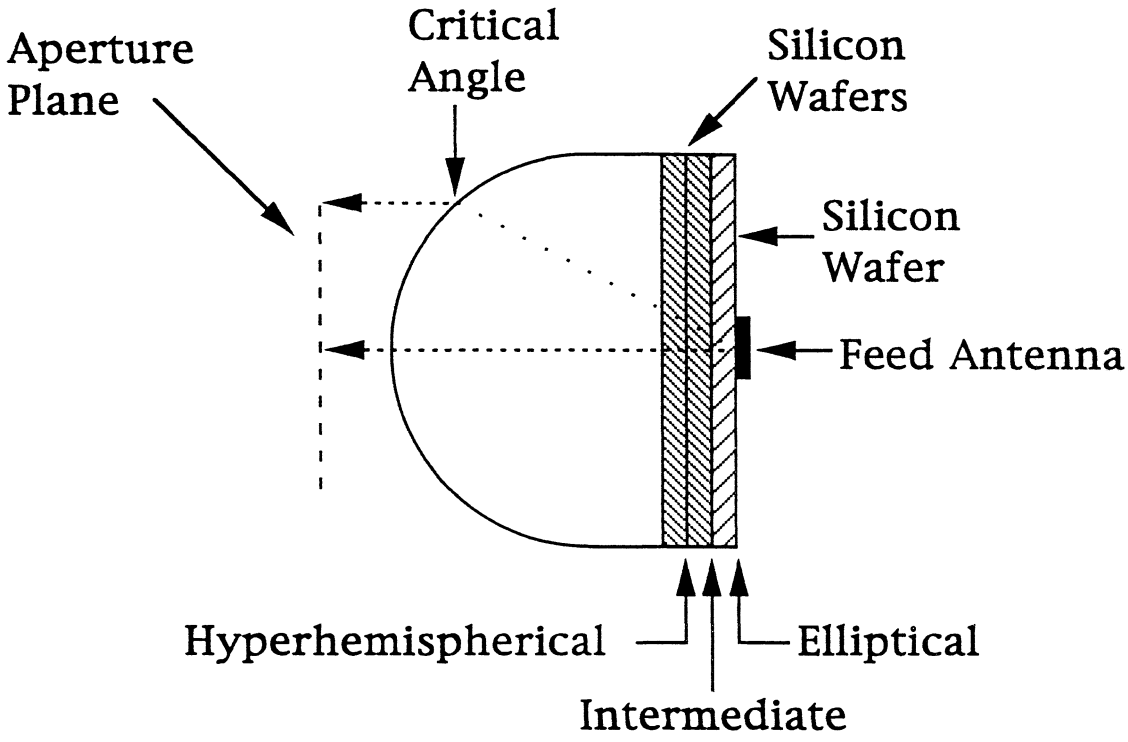

Figure 3: The ray-tracing method. Note the three focus positions that are achieved by adding high-resistivity silicon wafers.

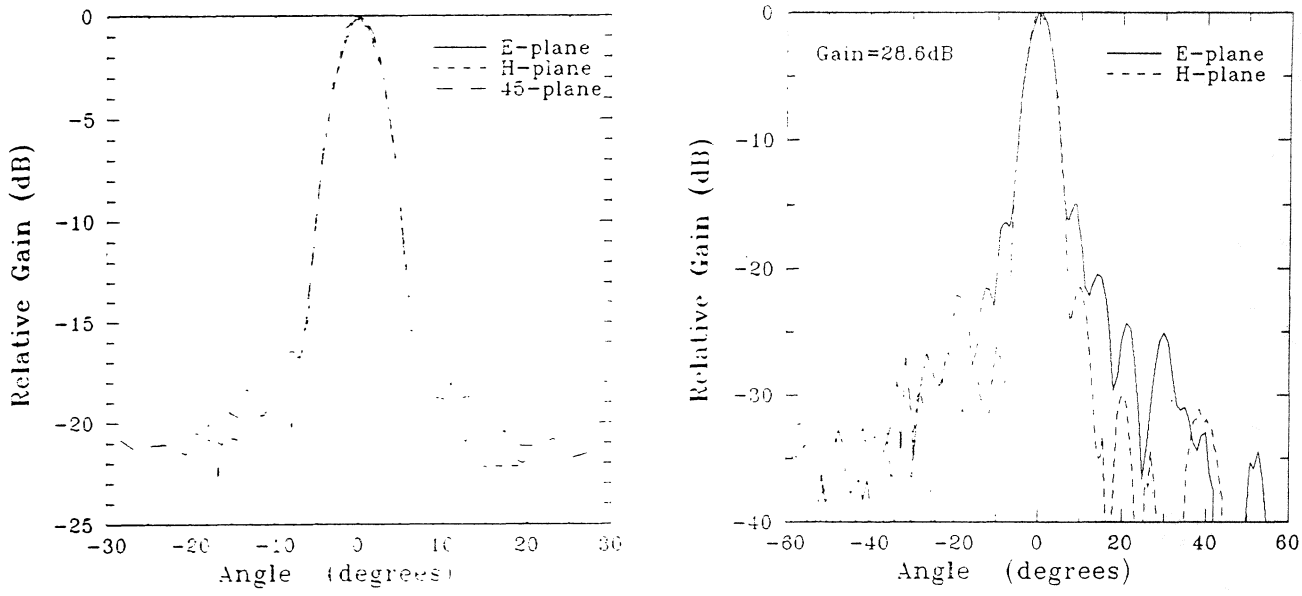

Figure 4: Measured patterns at the elliptical focus at 246GHz. The patterns are diffraction-limited by the size of the aperture

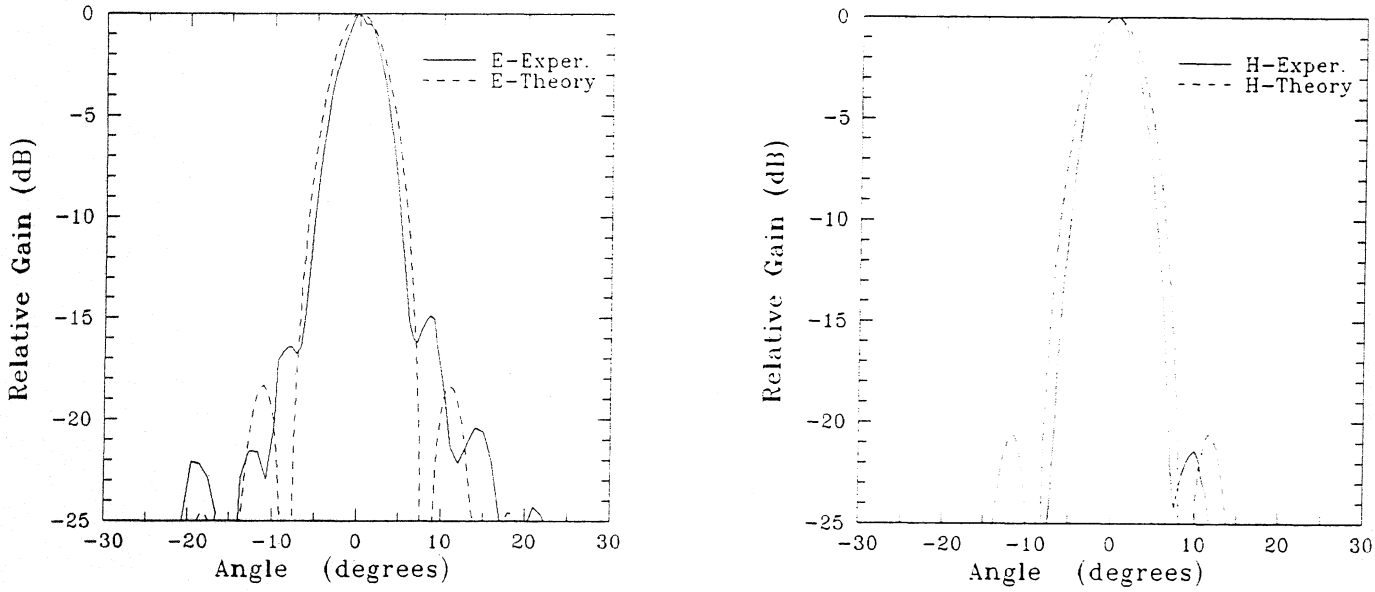

Figure 5: Comparison of theory vs. experiment for the elliptical focus. The critical angle limits the size of the aperture, resulting in wider theoretical patterns.

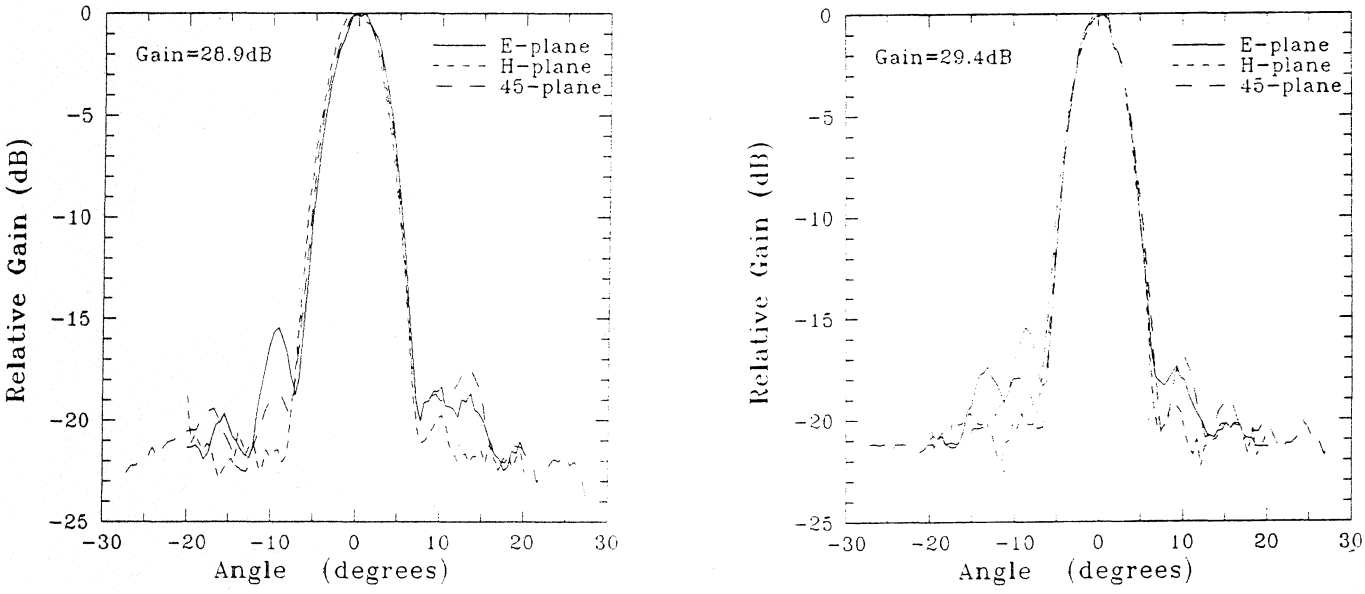

Figure 6: Measured patterns at the elliptical focus at 222GHz (left) and 270GHz (right).

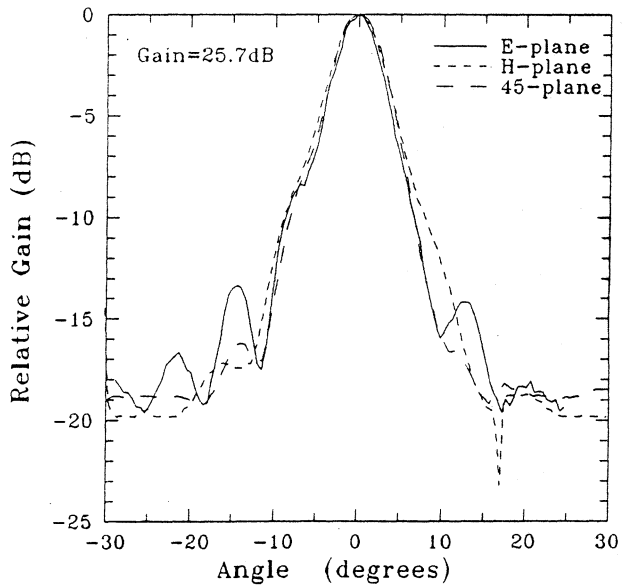

Figure 7: Measured patterns at the intermediate focus position at 246GHz.

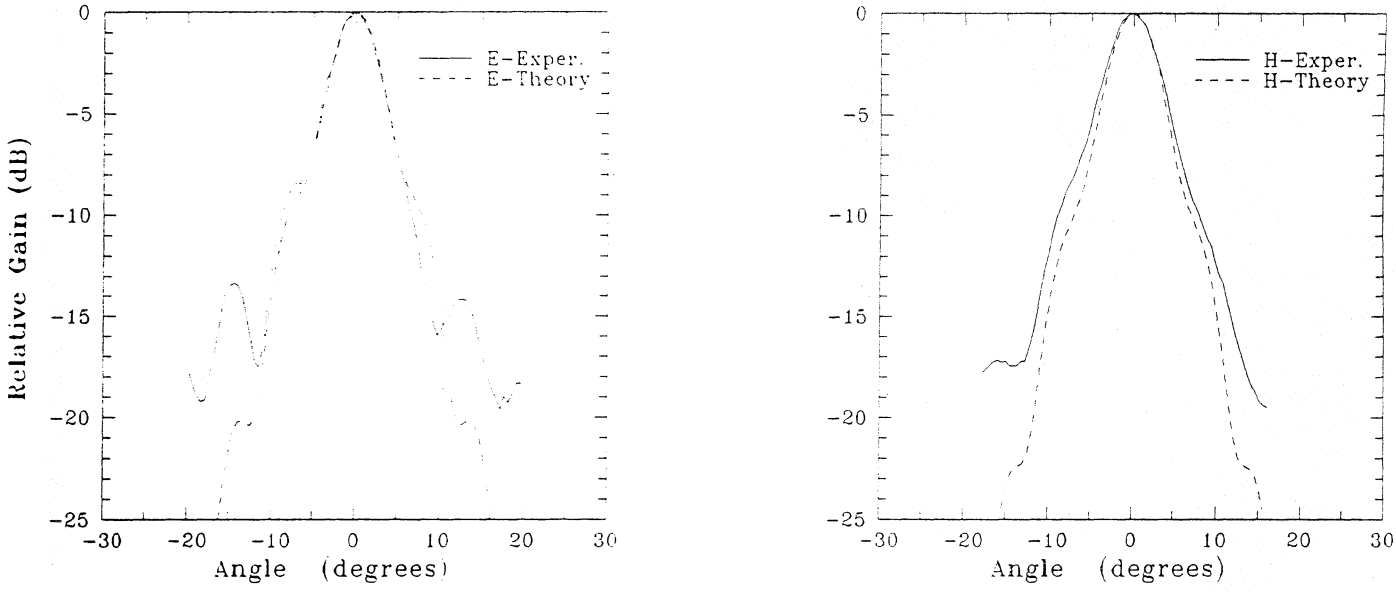

Figure 8: Comparison of theory vs. experiment for the intermediate focus.

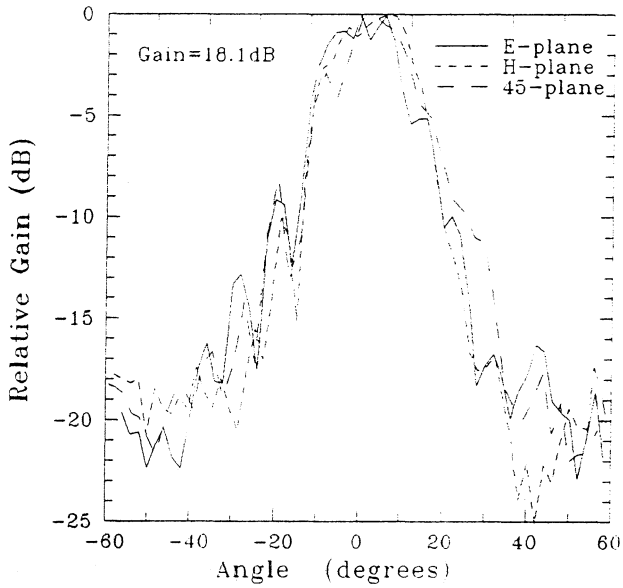

Figure 9: Measured patterns at the hyperhemispherical focus position at 246GHz.

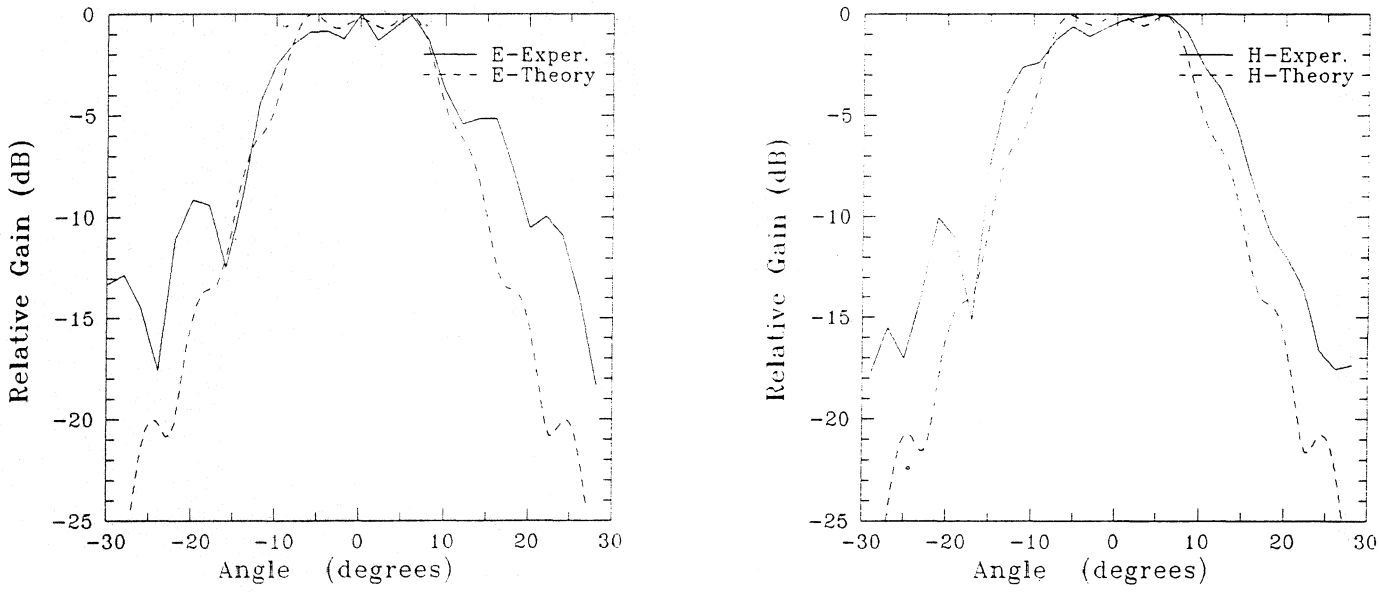

Figure 10: Comparison of theory vs. experiment for the hyperhemispherical focus. Notice the predicted multi-peak behaviour.

Coupling to Gaussian Beams

Focus Position (extension)	Gain	Gaussian Beam Parameters		Matching Efficiency
		Θ_0(amplitude)	Θ_1(phase)	
Elliptical (.39 radius)	28.6dB	5.0°	-	~ 79%
Intermediate (.32 radius)	25.7dB	8.2°	11.3°	~ 83%
Hyper-hemispherical (.25 radius)	18.1dB	13.3°	13.5°	~ 81%

Gaussian Beam Electric Field: $\exp[-(\Theta/\Theta_0)^2] \exp[j*\pi*(\Theta/\Theta_1)^2]$

$$\frac{\text{Max. Power Elliptical}}{\text{Max. Power Hyperhemispherical}} \cong 10\text{dB}$$

Figure 11: Table of Gaussian beam parameters.